Pathological post-mortem findings in lungs infected with SARS-CoV-2

The Journal of Pathology, Original Paper

PATHOLOGICAL POST MORTEM FINDINGS IN LUNGS INFECTED WITH SARS-COV 2

Stefania Damiani[1], Michelangelo Fiorentino[5], Alessandra De Palma[2], Maria Pia Foschini[2], Tiziana Lazzarotto[3], Liliana Gabrielli[3], Pier Luigi Viale[4], Luciano Attard[4], Mattia Riefolo[1], Antonia D'Errico[1]

From the Department of Pathology [1], Forensic Medicine [2], Microbiology [3], and Infectious Diseases [4], Azienda Ospedaliero-Universitaria di Bologna and the Department of Pathology [5] Bellaria-Maggiore Hospital, University of Bologna School of Medicine, Bologna, Italy

No conflicts of interest were declared

Running title: Autopsy lung findings in SARS-COV 2 deceased patients

Word count: 3727

Correspondence to: M Fiorentino, Department of Specialistic, Diagnostic and Experimental Medicine

University of Bologna, Via Massarenti 9, 40138 Bologna, Italy. E-mail: michelangelo.fiorentino@unibo.it

This article has been accepted for publication and undergone full peer review but has not been through the copyediting, typesetting, pagination and proofreading process, which may lead to differences between this version and the Version of Record. Please cite this article as doi: 10.1002/path.5549

Abstract

Italy was the first European nation to be massively infected by SARS-COV 2. Up to the end of May 2020 more than thirty-three thousand deaths had been recorded in Italy with a large prevalence among males, those over 75 years of age, and in association with co-morbidities. We describe the lung pathological and immunohistochemical post-mortem findings at the autopsy of 9 patients who died of SARS-COV 2 associated disease. We found in the lung tissues of all patients histological changes consistent with diffuse alveolar damage in various evolution phases ranging from acute exudative to acute proliferative to fibrotic phase. Alveolar damage was associated a prominent involvement of the vascular component in both the interstitial capillaries and in the mid-size vessels, with capillary fibrin micro-thrombi, as well as organized thrombi even in medium sized arteries, in most cases not related to sources of embolism. Eosinophilic infiltrate was also seen, probably reactive to pharmacological treatment. Viral RNA of SARS-COV 2 was detected from the lung tissues of all the nine patients. Immunohistochemistry for the receptor of the SARS-COV 2, ACE2, and its priming activatorTMPRSS2 revealed that both proteins co-localize in airway cells. In particular, the ACE2 protein was expressed in both endothelial cells and alveolar type I and II pneumocytes in the areas of histological diffuse alveolar damage (DAD). Pneumocytes but not endothelial cells also expressed TMPRSS2. There are no distinctive histological features of SARS-COV 2 infection with respect to SARS-COV 1 and other DAD with different aetiology. The identification of the cause of death in course of SARS-COV 2 infection is more likely multi-factorial.

Introduction

Coronaviruses are major pathogens for the human respiratory system. In the past, two outbreaks of coronaviruses (CoVs) have been reported. The severe acute respiratory syndrome (SARS)-CoV in 2002–2003 affected 8,422 people, mostly in PR China and Hong Kong, with 916 reported deaths and a mortality rate of 11%. The Middle East respiratory syndrome (MERS)-CoV in 2012 emerged in Saudi Arabia, affected 2,494 people, and killed 858 with a mortality rate of 34% [1]. In December 2019, a new outbreak occurred in the Chinese province of Hubei and in the City of Wuhan. The patients presented with symptoms of acute pneumonia including fever, cough, breathing difficulties, associated with diffuse lesions in both lungs. Chinese authorities stated that the causative agent was a novel coronavirus sharing some similarities with the (SARS)-CoV and it was named novel coronavirus 19 (Ncov-19) or SARS-COV 2 [2].

Italy was the second country to be massively infected by SARS-COV 2. The first patient diagnosed with SARS-COV 2 in Italy on February 18th was a 38-year-old healthy athlete from the city of Codogno (Lombardy) with no co-morbidities, who got infected from an unknown source. This patient "one" experienced severe acute respiratory syndrome and was admitted to an intensive care unit (ICU) and recovered after three weeks. Since then, the virus spread rapidly and particularly in Northern Italy with an exponential doubling time of infections and deaths. (3). To date (May 31st) about 233,000 Italians have been infected and more than 33,000 died of SARS-COV 2 (source Italian Ministry of Health). The

mean age of deceased patients was 80 years with a constant moderate predominance among men (6:4, M:F ratio). In severe cases, the most frequent symptoms in Italy were fever (76%), dyspnoea (72%), cough (38%), diarrhoea (6%). Most of the deceased patients died of acute distress respiratory syndrome (ARDS).

Airways represent the main target of SARS-COV 2. The entry of the coronavirus in the host alveolar cells is mediated by the angiotensin converting enzyme 2 (ACE2) and its receptor which are expressed in different organs (respiratory tract, heart, kidney, intestine and endothelial cells). The type II transmembrane serine protease TMPRSS2 cleaves and activates the spike protein (S) of both SARS-CoV and SARS-COV 2 for membrane fusion. In addition, the androgen-regulated *TMPRSS2* gene is capable of cleaving ACE2, thereby increasing the viral infectivity. While the pathogenesis of the coronavirus entry in the respiratory system is quite well understood, the pathological sequence of alveolar cell damage is still unclear, and patients experience different clinical behaviour not only according to the age and sex but also to previous co-morbidities such as obesity and diabetes. Recent reports on the course of SARS-COV 2 described variable clinical features ranging from overt ARDS to non-ARDS [4, 5]. The pathological damage in ARDS starts from an endothelial damage and progresses through the well-recognized evolution steps of interstitial oedema, alveolar damage, alveolar haemorrhage, and proliferation of type II pneumocytes. Finally, tissue repair occurs by collagen production and fibrosis [6, 7].

The histological aspects of lung injuries had been described for SARS-CoV2 [8, 9] and less frequently for MERS-CoV [10]. The main reported features were the presence of exudative and proliferative phases of diffuse alveolar damage (DAD) including endothelial damage, thrombosis of small and medium vessels and haemorrhagic foci up to infarcts. In some cases, associated bacterial pneumonia was described.

There are few detailed descriptions of the histological alveolar damage caused by SARS-COV 2. The occurrence of DAD with oedema, hyaline membranes and fibrosis are the most frequent described histological changes [11–14]. Wichmann, *et al* [15] reported twelve complete autopsies in German patients with SARS-CoV2. They found variable features of early phase DAD and diffuse pulmonary embolism which was considered the cause of death. In four cases they did not find DAD but only extensive and broncho-pneumonia like granulocytic infiltration of the alveoli and bronchi. In Italy, Carsana, *et al* [16] performed 38 partial autopsies on patients who died with SARS-COV 2 infection after a median of 16 days after the onset of symptoms. Histologically, they found modifications consistent with exudative and early proliferative phases of DAD. Finally, in the largest series of autopsy cases published to date on deceased patients with SARS-CoV-2, Edler, *et al* found variable pathological findings including DAD, purulent pneumonia, emphysema with destruction of alveolar septae, fibrosis, and lymphocytic infiltrates [17].

The Emilia-Romagna Region has been the second most important focus of SARS-COV 2 infection in Italy after Lombardy with over 27,000 infections and 4,000 deaths. Since the outbreak of the infection in our city of Bologna, we performed autopsies in patients with ascertained death from SARS-COV 2. Here we describe the postmortem pathological pulmonary findings in nine autopsy patients with different clinical course of SARS-COV 2-associated disease.

Patient Population and pathological examination

Nine full post-mortem autopsy examinations were performed at the S.Orsola and Bellaria Hospitals of the University of Bologna between 13th March and 17th April 2020, at the peak of the SARS-COV 2

infection in the Emilia-Romagna Region. All patients died of severe, progressive respiratory distress after being tested positive for SARS-COV 2 (pharyngeal swab). Patients undergoing PM examinations were selected according to either an age <60 years or an atypical clinical outcome. Autopsies were performed following the appropriate safety precautions suggested by the guidelines of the Istituto Superiore di Sanità [18] and the College of American Pathologists (https://www.cap.org/member-resources/councils-committees/cancer-topic-center/autopsy-topic-center). The examiners were equipped with personal protection devices (N-95 mask, disposable caps, face-shields, disposable body suits with shoe covers, gowns, gloves). Examinations took place in a negative-pressure autopsy room. Multiple samples from each lung were taken and fixed in 10% buffered formalin. Sections from the lung tissue were routinely stained with haematoxylin and eosin, Gram stain, Masson's Trichrome stain, and Periodic Acid/ Shiff. The study followed the Italian general rules used for scientific research purposes (regulation n.72–26/03/2012).

Immunohistochemistry

Routine immunohistochemical staining for wide-spectrum cytokeratin (AE1/AE3), TTF-1, p40, CD68, CD4/8, CD31, ERG, human cytomegalovirus (CMV), Herpes Simplex Viruses type 1 and 2 (HSV-1 and 2) were performed on a Benchmark-Ultra automated system (Ventana-Roche, Tucson, AZ, USA) using pre-diluted antibodies provided by the manufacturer. Immunohistochemistry for ACE2 was performed using antibody EPR44352 (diluted 1:1000; ab 108252 Abcam, Cambridge UK) and for TMPRSS2 with the antibody EPR3861 (diluted 1:6000; ab 92323 Abcam) both on the Benchmark-Ultra automated system.

Virological examination

Tissue sections cut at 10 µm thickness were placed in a 1.5 ml tube with 160 µl of Deparaffinization Solution (Qiagen, Hilden, Germany), 180 µl of tissue lysis buffer (ATL buffer, Qiagen) and 20 µl of protease (Proteinase K solution, Qiagen). After overnight incubation at 56 °C followed by 1 h of incubation at 90 °C, nucleic acids were extracted and purified using an ELITe InGenius® instrument with the ELITe InGenius SP 200 (ELITechGroup, Torino, Italy).

Qualitative detection of SARS-CoV-2 was accomplished using the GeneFinderTM COVID-19 PLUS RealAmp Kit (OSANG Healthcare, Anyang, Republic of Korea) and an ELITe InGenius® instrument. The kit detects RNA-dependent RNA polymerase (RdRp), envelope (E), and nucleocapsid (N) genes of SARS-CoV-2. The endogenous internal control allows confirmation the quality of the sample material extracted. The lowest concentration of SARS-CoV-2 that can be detected is 10 copies/reaction.

For the quantitative detection of CMV, Epstein Barr Virus (EBV) and human herpesvirus 6 (HHV-6) in the samples, the human DNA (hDNA) was quantified using a real-time PCR assay, Quantifiler® Human DNA Quantification Kit (Life Technologies, Waltham, MA, USA). Five nanograms of hDNA were processed for CMV, EBV, HHV-6-DNA quantification, using a real-time PCR assay, ELITe MGB™ kits (ELITech Group, Italy). Amplification, detection, and analysis were performed using a 7500 real-time PCR system (Applied Biosystems, Waltham, MA, USA). The tissue viral load was reported as number of viral copies/10 ng of hDNA. The lower limit of detection was 10 copies/10 ng of hDNA per PCR reaction.

Results

Clinical characteristics: Of the 9 patients, 8 were Caucasians and 1 was Indian; 7 males and 2 females. The mean age was 58 (range 44–70). All of our patients presented with fever, cough, shortness of breath and progressive dyspnoea, leading to mechanical ventilation and admittance into the ICU. All of

the nine patients were affected by co-morbidities and the most frequent were hypertension and being overweight - assessed by measure of the thickness of the umbilical sub-cutaneous tissue >8 cm. This ranged between 6.5 and 12 cm. Two patients had type II diabetes, two a previous history of stroke, one hemiplegia and chronic renal failure, one non-symptomatic Crohn's disease. The interval between the onset of SARS-COV 2 symptoms and death ranged from 6 to 35 days. During hospitalization four patients developed opportunistic bacterial infections *(Escherichia coli*, *Staphylococcus capitis* and *epidermidis*, *Pseudomonas aeruginosa*) and two tested positive for *Candida glabrata*. One patient (#6) was initially treated with extracorporeal membrane oxygenation (ECMO) then showed a clinical improvement that led to stopping the extracorporeal oxygenation and reduction of sedation. Five days after discontinuation of ECMO, the patient underwent rapid respiratory failure and died with high blood eosinophilia. Clinical data are summarized in Table 1.

Patients were treated from the onset of symptoms with variable antivirals: lopinavir/ritonavir (patients #2, #6, #7, #8), remdesivir (patient #2), oseltamivir (patients #6, #8), darunavir/cobicistat (patient #5). chloroquine (patients #2, #6) or hydroxychloroquine (patients #1, #2, # 3, #4, #5, #6, #7, #8, #9) were also used as per the protocol of our Institution. Several antimicrobials were also administered: azithromycin (patients #1, #2, #3, #4, #5, #6, #8), ceftriaxone (patients #2, #4, #5), piperacillin/tazobactam (patients #1, #2, #3, #4, #5, #6, #7, #8), linezolid (patients #2, #4, #6, #7, #8, #9), meropenem (patients #2, #6, #8, #9), daptomycin (patient #8), ertapenem (patient #9), ceftolozane/tazobactam (patient #9). Ceftriaxone and azythromycin were administered to every patient admitted with community acquired pneumonia as a part of our standard coverage antibiotic therapy. All the other antibiotics were variably prescribed for the treatment of opportunistic infection occurred during the ICU stay of each patient. Antimycotics (voriconazole) were used in patients #8 and #9). Immunosuppressive therapy was employed: in patients #2, #4, #5, #6 (tocilizumab), and in patients #1,

#9 (methylprednisolone). Patients with hypertension were treated with ramipril (patient #2), clonidine (patients #2, #5), esmolol (patient #6), metoprolol (patient #7). All patients were treated with enoxaparin, only patient #5 were treated in the last 4 days with calciparine and acetylsalicylic acid.

Pathological characteristics: At gross autopsy evaluation, the lungs of all patients were uniformly congested, purple-red and firm with occasional pink mildly crepitating areas at the apexes (patients #3 and #6). The weight of the lungs ranged from 1180 to 1390 grams. One patient (#4) had bilateral pulmonary artery thrombosis but we did not find thrombi in the iliac veins. Therefore, we assumed that thrombosis has formed *in situ*. We performed three random samples per lobe for a total of six samples for left lung and nine samples for right lung.

The histological features of the lung tissues from all our patients were consistent with DAD in various evolution stages depending upon the time from the disease onset. In all patients, the damage (exudative and/or reparative) involved from 50–100% of both lungs. We divided patients into three groups according to the histological phases of DAD [6] and the time-length of the disease from the onset of symptoms (<10 days; 11–20 days; >20 days). Histological features are summarized in Table 2.

Group 1: acute exudative phase

Only one patient was found in this phase. The patient (#1) died 6 days from the onset of symptoms (dry cough and fever). The lungs showed the typical histological changes of acute exudative phase of DAD. Alveolar spaces showed oedema, haemorrhage, and fibrin. Hyaline membranes (Figure 1) and more rarely ''fibrin balls'', like those typical of acute fibrinous organizing pneumonia, completely occluding the air spaces, were found [19]. Alveolar spaces were filled with desquamating pneumocytes and sparse macrophages. Pneumocytes were mostly of type I, necrotic and shed from the alveolar walls as evidenced by the immunostaining for AE1/AE3 Cytokeratin and TTF-1. No atypical or cytopathic

changes were seen in the pneumocytes (cytomegaly, nucleomegaly, clearing of nuclear chromatin or prominent nucleoli). The interstitial space showed vascular congestion with markedly ''open'' capillaries with frequent small hyaline micro-thrombi (Figure 1 inset). The inflammatory infiltrate was composed predominantly of neutrophilic granulocytes and less frequent monocytes.

Large venous vessels showed thrombotic material containing small aggregates of mycotic spores consistent with *Candida glabrata*.

Group 2: sub-acute proliferative phase

Four patients (#2, #3, #4, #5) showed histological changes consistent with subacute florid proliferative phase of DAD. In these cases, the predominant features were multiple foci of fibroblastic proliferation with many thin bands of fibrotic tissue, highlighted by Masson's trichrome staining (Figure 2A). Areas of squamous metaplasia, immunoreactive for p40, were seen in all four patients and this feature was prominent in one case (#2) (Figure 2B). Shed type II pneumocytes showed viral-like changes with frequent cytomegaly and prominent nucleoli. However, none of these cells turned out positive for CMV and HSV-1 and 2. Some type II pneumocytes had a very large amphophilic cytoplasm containing small bluish particles, reminiscent of the Nissl bodies observed in neurons, that might represent enlarged rough endoplasmic reticulum (Figure 2 inset). Along with the proliferation of both the epithelial and the connective components of alveolar septa, patients in this group still showed focal evidence of persistent acute damage with fibrin hyaline membranes and sparse fibrin balls (Figure 2C) which were positive on PAS staining and also immunoreactive for cytokeratin . Prominent vascular alterations in small to medium sized vessels were observed in all the patients of this group. We noticed thrombi in many capillaries and small venules and arteries, sometimes with evidence of recanalization. These features were particularly prominent in patients #2 and #5. In patients, all patients in this group had

areas of necrotic lung consistent with red infarction (Figure 3). Interstitial inflammation in this group mainly consisted of CD4+ lymphocytes. All patients in this group showed rare interstitial eosinophils.

Group 3: late fibrotic disease:

Four patients (#6,#7,#8,#9) showed features of a more advanced proliferative phase of DAD. This finding was in keeping with the longer time length of disease in these patients (>20 days). Areas of well-formed dense fibrotic bands were seen and involved about the 50% of the examined lung samples in three patients and over 75% in one (#9). Loose fibroblastic proliferation was evident, but usually not so marked and diffuse as in Group 2. Foci of acute damage (oedema, fibrin, hyaline membranes) were still present even in these ''late'' patients. However, the histologic signs of repair, i.e. dense fibrosis and loose fibroblastic proliferation, overwhelmed acute damage (Figure 4). In addition, this group of patients showed fibrin thrombi in small and medium sized vessels, areas of infarction and proliferating capillaries in the alveolar septa. The case #8 showed a unique feature with abnormal proliferation of small capillaries that expanded into the alveolar septa resembling a glomeruloid appearance, as stated by CD31 and ERG immunostaining (Figure 5). The endothelial cells in these areas had prominent, slightly hyperchromatic nuclei, but no atypical or ''viral-like'' appearance. Patients #6, #8 and #9 also displayed typical bacterial bronchopneumonia with a bronchocentric neutrophilic infiltrate. Patients #6 and #9 showed diffuse infiltration of eosinophilic granulocytes, consistent with acute eosinophilic pneumonia. Patient #6 had superimposed infections from *E. coli* while #8 and #9 from *P. aeruginosa* with microthrombi and diffuse blood extravasation and hemosiderin-laden macrophages typical of this infection. The lung tissues of the patients in Groups 2 and 3 showed scattered multinucleated giant cells of two types: 1) some were CK- and CD68+ resembling foreign body reaction cells; 2) other were CK+, syncytial-like, with large nuclei and viroid appearance.

Immunohistochemistry for ACE2 and TMPRSS2 revealed that both proteins co-localized in airway cells. In particular, the ACE2 protein was expressed in both endothelial cells and alveolar type I and II pneumocytes. Pneumocytes but not endothelial cells also expressed TMPRSS2 protein. Both ACE2 and TMPRSS2 were also co-expressed in shed alveolar cells in the areas of histological DAD (Figure 6).

Virological results: The RNA of SARS-COV 2 was detected in lung tissues of both or at least one lung of all nine patients; results are summarized in Table 3.

Regarding the tissue detection of the herpesviruses, all lungs were negative for CMV-DNA, and negative (or showed very low number of copies) for EBV and HHV6-DNA (<10 copies/10ng hDNA) (Table 3). These findings confirm that the lung tissues may harbour latent EBV and HHV6 infections.

DISCUSSION

The clinical and histological lung injury from SARS-COV 2 is still matter of debate. The report published to date described features ranging from overt DAD to vascular damage probably mediated by complement activation. The autopsy reports are quite heterogeneous in terms of number of patients, type of samples, clinical course, and treatments [11–17, 20].

We performed a full pathological PM study of the lung tissues of 9 patients who died with ascertained SARS-COV 2 infections. The main pathological finding in all our patients was acute lung injury with variable signs of repair according to the duration of disease. As expected, the single patient with illness lasting <10 days (Group 1) showed a predominantly acute exudative pattern with diffuse hyaline membrane or fibrin balls formation and scanty repair. A limitation of our autopsy series is that the cases were not consecutive deaths for SARS-COV 2, but rather the autopsy was requested by clinicians, due to an expected worsening of the disease. An additional limitation of our study is the presence of just one patient in the Group 1. However, the data from other series confirm this type of lung damage

in patients with early phase of SARS-COV 2 infection (11, 12, 14). In the eight patients with sub-acute proliferative phase (10–20 days, Group 2) and late fibrotic phase (more than 25 days, Group 3) of DAD, histological consistent features were found [6]. These findings are largely in keeping with those previously reported for SARS-Cov 1 and in early reports for SARS-COV 2 [8,9,11–14].

Interstitial fibrosis involved 50% of the lung in three, and more than 75% in one, of the patients of Group 3. This extensive remodelling of lung tissue may lead one to speculate a rapid course towards honeycombing transformation. A series of 38 SARS-COV 2 patients from two hospitals in Lombardy reported the prevalence of exudative over fibrotic phases of DAD, possibly due to the short duration of the disease in their patients (16). Although the histology of resolving DAD in surviving patients is not well documented, it is known that patients with significant amount of fibrosis may undergo persistent restrictive impairment (6). However, the variable clinical course of the patients described by us and elsewhere prevents the drawing of certain conclusions on the fibrotic evolution in SARS-COV 2 patients, at least to date.

Five patients belonging to Groups 2 and 3 (#3, #4, #5, #7, #8) showed scattered eosinophils in the alveolar interstitium. Two additional patients from Group 3 (#6 and # 9) revealed features consistent with actual eosinophilic acute pneumonia. One of the latter (# 6) also developed high blood eosinophils after 21 days from the clinical onset of the respiratory disease. Some of the drugs administered to these patients have been previously associated with the onset of eosinophilic pneumonia [21,22]. We believe that the presence of eosinophils or true eosinophilic pneumonia in our patients with long-standing disease could reflect a reaction to therapy (i.e. to hydroxychloroquine or tazobactam) rather than a SARS COV2 related alteration.

The vascular injury and the presence of micro-thrombi has been reported as a peculiar trait of SARS-COV 2 infection not only in the lung, but also in systemic vessels [5,23,24]. SARS-COV1 patients described by Hwang, *et al* [8] also showed prominent vascular damage with thrombi, endothelial denudation, and infarcts. However, they found that the vascular injury was prominent also in "control DAD SARS COV1 negative cases". Wichmann, *et al* found early-phase DAD in 8/12 cases although in 4 cases the cause of death was due to pulmonary diffuse embolism; the remaining 4 patients showed a diffuse granulocyte infiltration along the alveoli ad bronchial wall [15]. Carsana, *et al* [16] describing the typical findings of DAD in their SARS-COV 2 patients found a significant number of thrombi in capillaries and medium sized arteries, highlighting the correlation between thrombotic phenomena and the severity of SARS-COV2. In our series, we confirm the presence of diffuse thrombosis in small and medium size arteries, although just one patient showed evidence of bilateral massive pulmonary thrombo-embolism.

In addition, we have seen a prominent involvement of the vascular component in both the interstitial capillaries and in the mid-size vessels. Accordingly, our patients showed capillary fibrin micro-thrombi, as well as organized thrombi even in medium sized arteries. In one patient (patient #8) we found a marked capillary proliferation in the septal interstitium, featuring a glomeruloid appearance (Figure 5), and resembling pulmonary capillary angiomatosis [24]. Ackermann, *et al* [25] studied a series of 7 autopsy lungs in SARS-COV2 patients, comparing the histology of these patients with those of patients who died with H1N1-related DAD. They found more extensive endothelial damage and thrombi in SARS-COV2 lungs and an angiogenesis index 2.7 times higher compared to non-SARS-COV2 patients. Endothelial cells play a crucial role in the development of acute lung injury. Electron microscopy can reveal damage in cytoplasmic membrane of alveolar endothelial cells leading to alterations of vascular permeability, fluid accumulation and recruitment of neutrophils and macrophages [6, 7, 27,28].

Therefore, a vascular damage exists in any DAD regardless the underlying cause. However, we can argue that in SARS-COV 1/2-related diseases these features seem more pronounced than in acute lung injury of other aetiologies.

We demonstrate for the first time by immunohistochemistry the presence of ACE2 and TMPRSS2 in the alveolar damaged cells of patients with SARS-COV 2 infection. ACE2 and TMPRSS2 proteins act in synergy allowing the attachment and the entry of the SARS-COV 2 in airway cells [29]. We have found the presence of the two proteins in type II pneumocytes shed in the alveoli of DAD as well in newly formed interstitial capillaries. In virus-induced DAD, viral particles are found usually in type 2 pneumocytes [6]. In our series, patients in Groups 2 and 3 (subacute proliferative and late fibrosing phases) showed atypical type 2 pneumocytes with "viroid", cytopathic, appearance and cytoplasmic bluish granules. Varga, *et al* [30] reported evidence of direct viral infection of endothelial cells in three covid-19 patients. These findings could be of great relevance given the in vitro anti-viral activity of the selective TMPRSS2 inhibitor camostat [31].

The thorough histological evaluation of lungs with severe SARS-COV 2 infection in our series confirms the presence of DAD in different evolution phases associated with variable co-morbidities and super-infections.

The identification of the cause of death in course of SARS-COV 2 infection is more likely multi-factorial and possibly includes a severe systemic inflammatory response syndrome.

We conclude that there are no pathognomonic, distinctive histological features of SARS-COV 2 infection with respect to SARS-COV 1 and other DAD of different aetiology, however, there is no doubt that in SARS-COV 2 patients the vascular phenomena, i.e. endothelial damage, thrombosis and angiogenesis

appear more pronounced, and therefore an important role of endothelial factors can be speculated, as suggested by Ackermann, *et al* [26].

AUTHOR CONTRIBUTIONS STATEMENT

SD and AD: study design. AD, MPF and ADP: performed the autopsies. SD, AD, ADP, MR and MPF generated and analyzed pathology data. LA and PLV provided the clinical data. TL and LG provided the microbiological data. MF, SD and AD wrote the paper and critically reviewed the data.

REFERENCES

1. Singhal T: A review of coronavirus disease-19 covid-19. In J pediat 87(4): 281-286, 2020
2. Wang D., Hu B., Hu C., Zhu F., Liu X., Zhang J., Wang B., Xiang H., Cheng Z., Xiong Y., Zhao Y., Li Y., Wang X., Peng Z.: Clinical Characteristics of 138 Hospitalized Patients With 2019 Novel Coronavirus–Infected Pneumonia in Wuhan, China. Jama 7: 1061-1069, 2020.
3. Grasselli G., Zangrillo A., Zanella A., Antonelli M., Cabrini L., Castelli A., Cereda D., Coluccello A., Foti G., Fumagalli R., Iotti G., Latronico N., Lorini L., Merler S., Natalini G., Piatti A., Ranieri M.V., Scandroglio A.M., Storti E., Cecconi M., Presemt A: for the COVID-19 Lombardy ICU network. JAMA, 6:81-88, 2020
4. Gattinoni L, Coppola S, Cressoni M, Busana M, Rossi S, Chiumello D. COVID-19 Does Not Lead to a "Typical" Acute Respiratory Distress Syndrome. *Am J Respir Crit Care Med*. 2020;201(10):1299-1300.
5. Magro C, Mulvey JJ, Berlin D, et al. Complement associated microvascular injury and thrombosis in the pathogenesis of severe COVID-19 infection: A report of five cases. *Transl Res*. 2020;220:1-13.
6. Leslie KO and Wick MR: Practical Pulmonary Pathology. Churchill Livingstone 2005
7. Thomashefski JF, Cagle PT, Farver CF and Fraire AE: Dail & Hammar's Pulmonary pathology Vol I. 3rd ed. Springer, 2008
8. Franks TJ, Chong PY, Chui P, et al: Lung pathology of severe acute respiratory syndrome (SARS): a study of 8 autopsy cases from Singapore. Hum Pathol 34: 743-748, 2003
9. Hwang DM, Chamberlain DW, Poutanen SM et al: Pulmonary pathology of severe acute respiratory sybdrome in Toronto. Mod Pathol 18: 1-10, 2005

10. Bradley BT and Bryan A: Emerging respiratory infections: The infectious disease pathology of SARS, MERS, pandemic influenza, and Legionella Sem Diagn Pathol 36: 152-159, 2019
11. Xu Z, Shi L, Wang Y, et al. Pathological findings of COVID-19 associated with acute respiratory distress syndrome [published correction appears in Lancet Respir Med. 2020 Feb 25;:]. *Lancet Respir Med*. 2020;8(4):420-422.
12. Barton LM, Duval EJ, Stroberg E, Ghosh S, Mukhopadhyay S. COVID-19 Autopsies, Oklahoma, USA [published correction appears in Am J Clin Pathol. 2020 May 5;153(6):852]. *Am J Clin Pathol*. 2020;153(6):725-733.
13. Zhang H, Zhou P, Wei Y, et al. Histopathologic Changes and SARS-CoV-2 Immunostaining in the Lung of a Patient With COVID-19. *Ann Intern Med*. 2020;172(9):629-632.
14. Tian S, Hu W, Niu L et al : Pulmonary pathology of early-phase 2019 novel coronavirus (COVID-19) pneumonia in two patients with lung cancer. J Thorac Oncology 15(5): 700-704, 2020
15. Wichmann D, Sperhake JP, Lütgehetmann M, et al. Autopsy Findings and Venous Thromboembolism in Patients With COVID-19: A Prospective Cohort Study. *Ann Intern Med*. 2020;173(4):268-277.
16. Carsana L, Sonzogni A, Nasr A, et al. Pulmonary post-mortem findings in a series of COVID-19 cases from northern Italy: a two-centre descriptive study [published online ahead of print, 2020 Jun 8]. *Lancet Infect Dis*. 2020;S1473-3099(20)30434-5.
17. Edler C, Schröder AS, Aepfelbacher M, et al. Dying with SARS-CoV-2 infection-an autopsy study of the first consecutive 80 cases in Hamburg, Germany [published correction appears in Int J Legal Med. 2020 Jun 19;:]. *Int J Legal Med*. 2020;134(4):1275-1284.

18. Gruppo di lavoro ISS Cause di morte COVID-19. Procedura per l'esecuzione di riscontri diagnostici in pazienti deceduti con infezione da SARS-CoV-2. Versione del 23marzo 2020.Roma: Istituto Superiore di Sanità; 2020 Rapporto ISS COVID-19, n.6/2020
19. Beasley MB, Franks TJ, Galvin JR et al: Acute fibrinous and organizing pneumonia. A histologic pattern of lung injury and possible variant of diffuse alveolar damage. Arch Pathol Lab Med 126: 1064-70, 2002
20. Tian S, Xiong Y, Liu H, et al. Pathological study of the 2019 novel coronavirus disease (COVID-19) through postmortem core biopsies. *Mod Pathol*. 2020;33(6):1007-1014.
21. Ishiguro Y, Muro Y, Murase C et al.: Drug-induced acute eosinophilic pneumonia due to hydroxychloroquine in a chilblain lupus patient.J Dermatol. 2019 Oct;46(10):e356-e35
22. García-Moguel I, Bobolea I, Diéguez Pastor MC et al: Acute eosinophilic pneumonia due to piperacillin/tazobactam. Ann Allergy Asthma Immunol. 2019 Mar;122(3):334-336
23. Zhang Y, Xiao M, Zhang S, et al. Coagulopathy and Antiphospholipid Antibodies in Patients with Covid-19. *N Engl J Med*. 2020;382(17):e38.
24. Lillicrap D: Disseminated intravascular coagulation in patients with 2019-nCov pneumonia. J Thromb Haemost. 2020 Apr;18(4):786-787.
25. O'Keefe MC, Post MD: pulmonary capillary hemangiomatosis: a rare cause of pulmonary hypertension. Arch Pathol Lab Med. 2015 Feb;139(2):274-7.
26. Ackermann M, Verleden SE, Kuehnel M, et al. Pulmonary Vascular Endothelialitis, Thrombosis, and Angiogenesis in Covid-19. *N Engl J Med*. 2020;383(2):120-128.
27. Katzenstein A-L A: Katzenstein and Askin's Surgical Pathology of non-neoplastic lung diseases. Series Major Problems in Pathology 4th ed.Saunders, 2006

28. Travis WD, Colby TV, Koss MN et al : Non-neoplastic disorders of the lower respiratory tract. Series Atlas of Non-tumor Pathology, AFP 2002
29. Hoffmann M, Kleine-Weber H, Schroeder S, et al. SARS-CoV-2 Cell Entry Depends on ACE2 and TMPRSS2 and Is Blocked by a Clinically Proven Protease Inhibitor. *Cell*. 2020;181(2):271-280.
30. Varga Z, Flammer AJ, Steiger P, et al. Electron microscopy of SARS-CoV-2: a challenging task - Authors' reply [published online ahead of print, 2020 May 19]. *Lancet*. 2020;S0140-6736(20)31185-5.
31. Matsuyama S, Nao N, Shirato K, et al. Enhanced isolation of SARS-CoV-2 by TMPRSS2-expressing cells. *Proc Natl Acad Sci U S A*. 2020;117(13):7001-7003.

LEGENDS TO FIGURES

Figure 1.Acute exudative phase DAD showing oedema and hyaline membrane formation (original magnification 100x). Inset: alveolar capillaries are congested and filled with hyaline thrombotic material (original magnification 200x).

Figure 2. Subacute proliferative DAD (A) alveolar septa are enlarged by proliferating fibroblast bodies and lympho-plasmacytic infiltration (Trichrome stain, original magnification 200x). Inset: type 2 pneumocytes have large ''viroid'' nuclei and large amphophilic cytoplasm containing small bluish particles, reminiscent of the Nissl bodies observed in neurons (original magnification 200x). (B) Foci of squamous metaplasia are evident (original magnification 100x). (C) proliferative DAD with foci of persistent acute damage. Alveolar septa are lined by type 2 pneumocytes with prominent nuclei and the alveolar spaces are filled with "fibrin balls" (arrows) (original magnification 100x).

Figure 3. Thrombi in medium sized vessels and haemorrhagic infarct were present mainly in patients from Groups 2 and 3 (original magnification 100x).

Figure 4. Dense fibrosis was the most prominent feature in Group 3 patients (Trichrome stain, original magnification 200x).

Figure 5. Patient #8: proliferation of small capillaries that expanded into the alveolar septa with a glomeruloid appearance, resembling pulmonary angiomatosis. Upper inset: endothelial cells are positive with the ERG antibody. Lower inset: staining for CD31 highlights the glomeruloid appearance of alveolar capillaries (original magnification 200x).

Figure 6. Immunohistochemistry for ACE2 (left) and TMPRSS2 (right) in a case of diffuse alveolar damage caused by SARS-COV2. Single arrows indicate type I and type II positive pneumocytes. Double arrows indicate endothelial positive cells. (DAB, original magnification 200x).

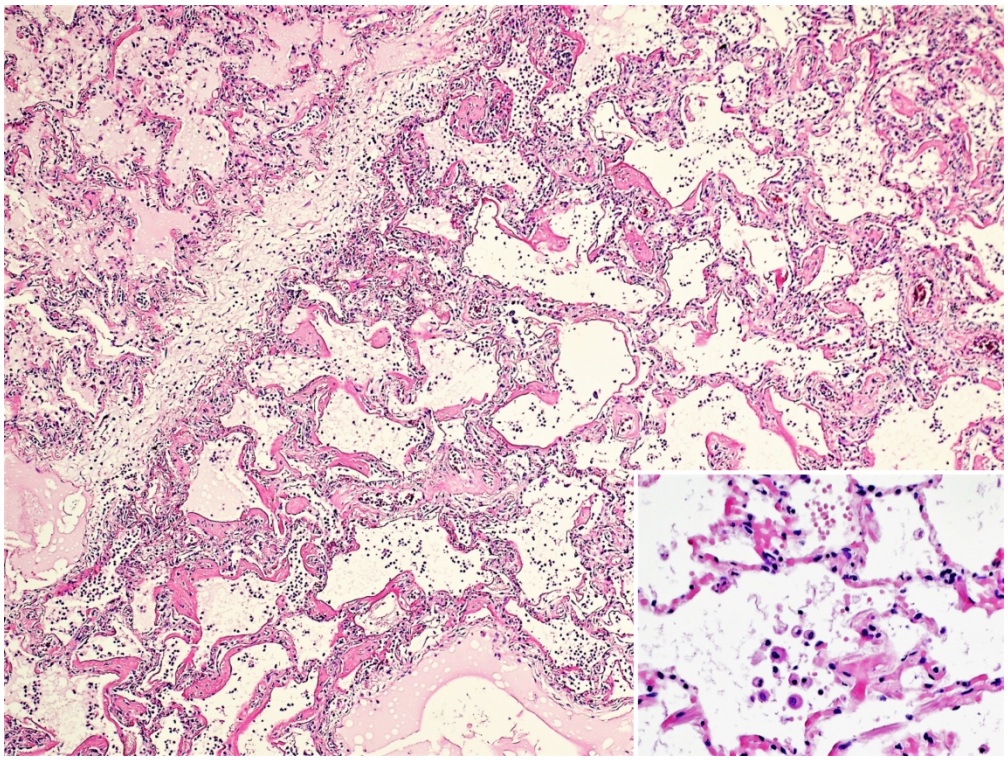

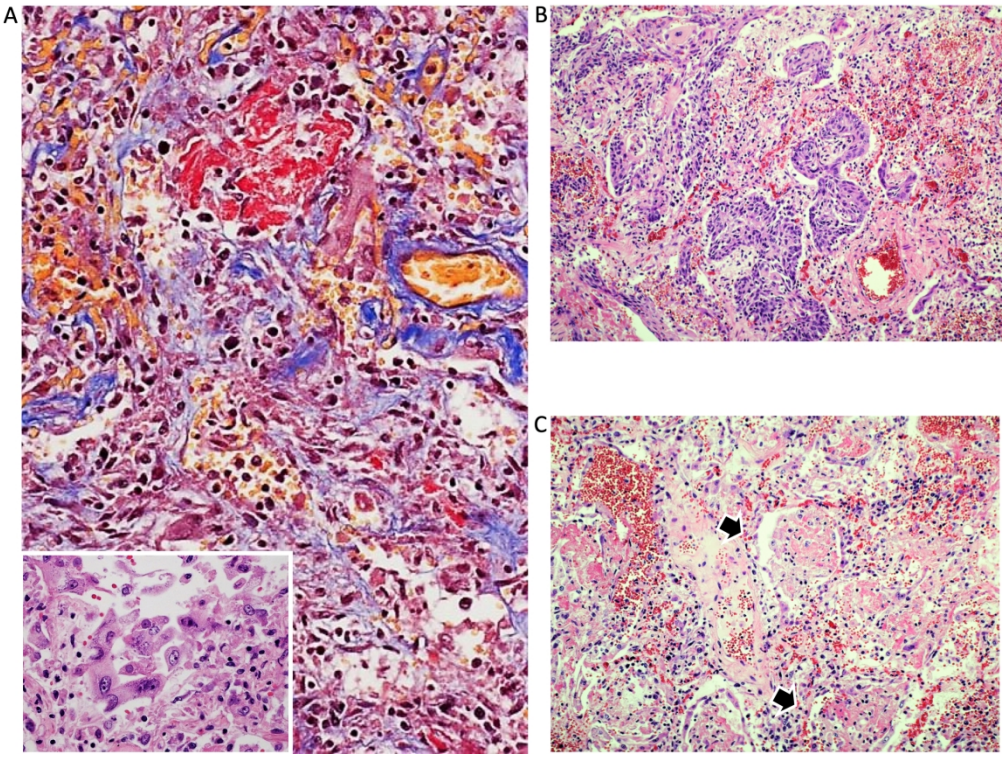

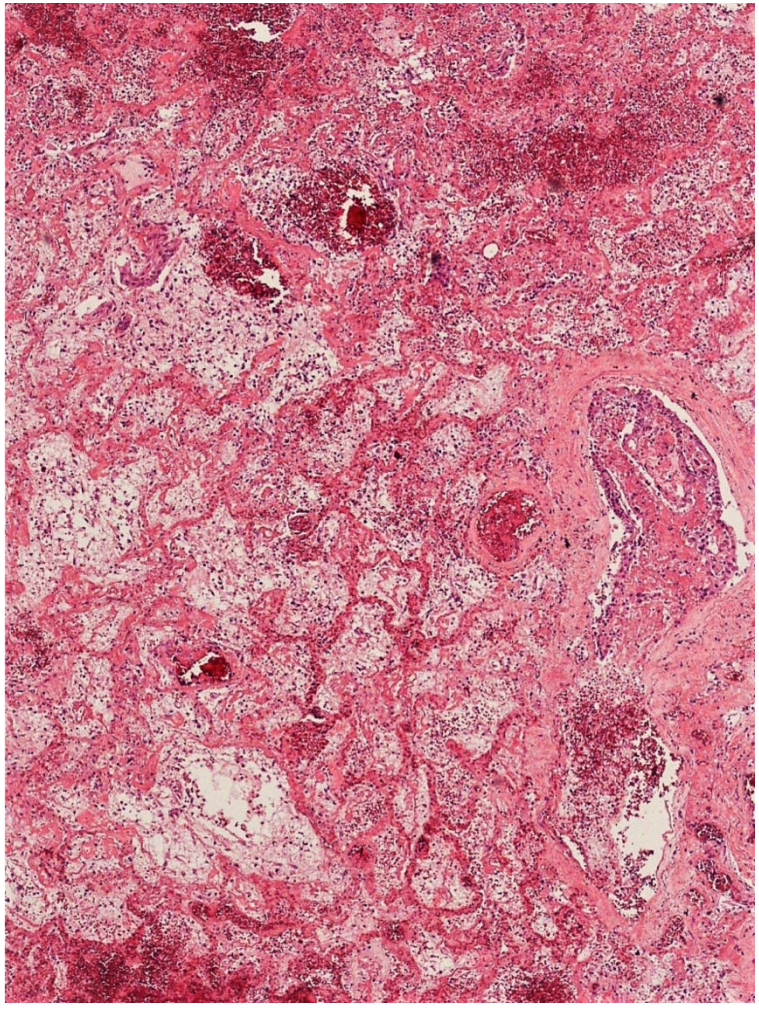

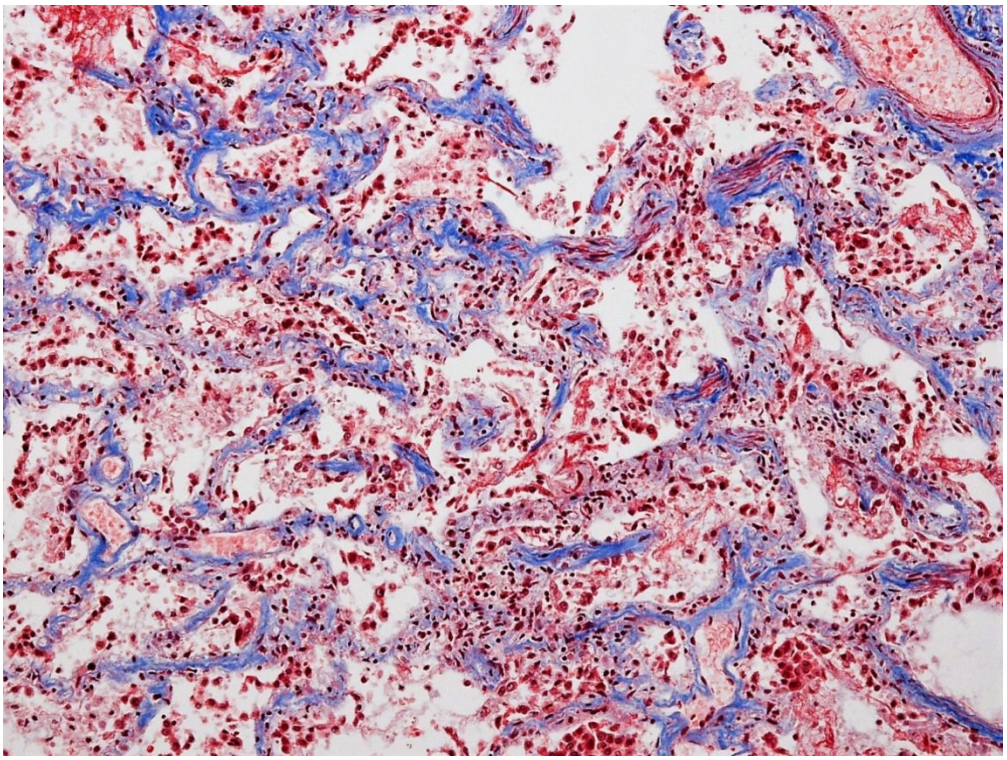

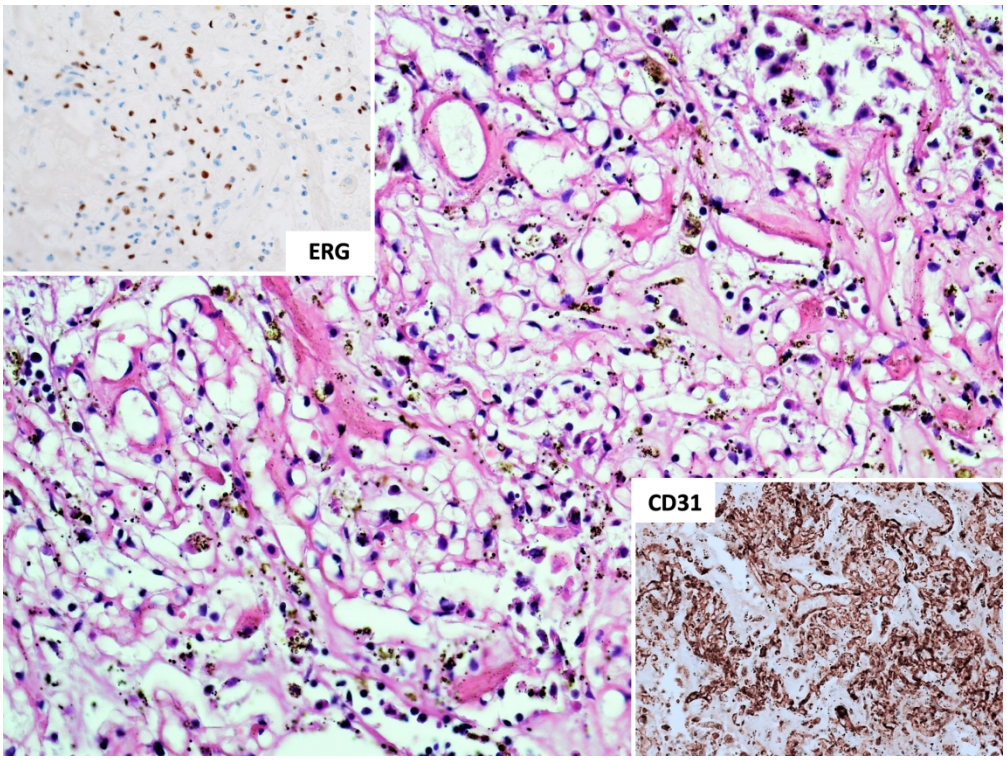

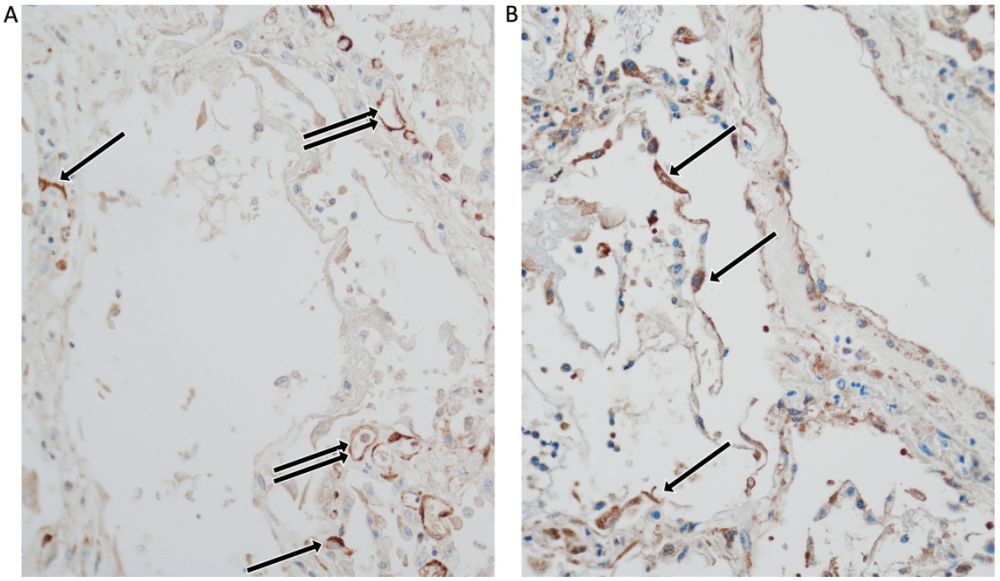

Table 1: Clinical data

Patient	Sex	Age (years)	Symptoms duration before death (days)	Detected microorganisms	Comorbility			
					Overweight	Hyper-tension	Diabetes mellitus	Other
#1	M	51	6	*Candida glabrata*	No	Yes	No	previous stroke (hemiplegy) chronic renal failure (dialysis)
#2	M	64	16	-	Yes	Yes	No	-
#3	F	70	13	-	Yes	Yes	No	previous stroke
#4	M	62	14	-	Yes	Yes	No	-
#5	M	52	17	-	Yes	Yes	No	-
#6	M	44	26	*Escherichia coli*	Yes	Yes	Yes	-
#7	F	64	25	*Candida glabrata*	Yes	Yes	No	Crohn's disease
#8	M	50	32	*Staphylococcus aureus, Candida albicans, Staphylococcus capitis, Pseudomonas aeruginosa*	Yes	Yes	Yes	-
#9	M	66	35	*Pseudomonas aeruginosa, Staphylococcus epidermidis, Candida glabrata,*	No	Yes	No	dyslipidaemia

Table 2: Histological features (summarized in percentage of tissue involvement: 1 up to 25%; 2 up to 50%; 3 up to 75%; 4 up to 100%)

Patient	Airspace oedema	Airspace haemorrhage and congestion	Fibrin (hyaline membranes, loose fibrin and fibrin balls)	Loose fibroblastic bodies	Type 2 pneumocyte hyperplasia with cytopathic features	Microscopic thrombi	Infarcts	Capillary proliferation	Dense fibrosis	Bacterial pneumonia	Eosinophils
Group 1. ***Acute exudative phase*** *(<10 days)*											
#1	3	2	2	1	-	1	-	-	no	none	none
Group 2. ***Subacute proliferative phase*** *(11–20 days)*											
#2	1	2	3	4	2	3	2	1	2		rare
#3	1	1	2	*2*	2	2	1	1	1		rare
#4	1	2	2	3	1	2	1	1	2		rare
#5	1	2	3	3	2	3	2	2	2		rare
Group 2. ***Late fibrotic phase*** *(>20 days)*											
#6	1	2	1	2	2	2	2	2	2	yes	eosinophilic pneumonia
#7	1	2	1	2	3	2	1	1	2	no	rare
#8	1	1	2	2	3	3	2	3	2	yes	rare
#9	1	1	2	*1*	2	3	2	2	4	yes	eosinophilic pneumonia

Table 3. Virological assessment of patients' lung tissues.

PATIENT	RIGHT LUNG				LEFT LUNG			
	SARS-COV2 RNA	CMV-DNA copies/10ng	EBV copies/10ng	HHV6 copies/10ng	SARS-COV2 RNA	CMV copies/10ng	EBV copies/10ng	HHV6 copies/10ng
#1	positive	negative	negative	positive <10	positive	negative	negative	positive <10
#2	positive	negative	negative	negative	positive	negative	negative	negative
#3	positive	negative	negative	negative	positive	negative	negative	negative
#4	positive	negative	negative	negative	positive	negative	negative	negative
#5	positive	negative	negative	negative	positive	negative	negative	positive <10
#6	positive	negative	positive <10	negative	negative	negative	positive <10	positive <10
#7	positive	negative	positive <10	negative	negative	negative	positive <10	negative
#8	positive	negative	negative	positive <10	positive	negative	negative	negative
#9	negative	negative	negative	negative	positive	negative	positive <10	negative